2. Forster, T. 1948. Zwischenmolekulare Energiewanderung und Fluoreszenz. *Ann. Physik* 2:55–75.
3. Steinberg, I. Z., and E. Katchalski. 1968. Theoretical analysis of the role of diffusion in chemical reactions, fluorescence quenching, and nonradiative energy transfer. *J. Chem. Phys.* 48:2404–2410.
4. Stender, W., and K. H. Scheit. 1977. Studies of the topography of the binding site of DNA-dependent RNA polymerase from *E. coli* for the anitbiotic rifamycin SV. *Eur. J. Biochem.* 76:591–600.
5. Dexter, D. L. 1953. A theory of sensitized luminescence in solids. *J. Chem. Phys.* 21:836–850.

# POSSIBLE DISTORTION OF ANTIBODY BINDING SITE OF THE Mcg BENCE-JONES PROTEIN BY LATTICE FORCES

M. Schiffer, *Division of Biological and Medical Research, Argonne National Laboratory, Argonne, Illinois 60439 U.S.A.*

The Mcg Bence-Jones protein dimer closely resembles an antigen binding fragment of a functional antibody molecule both in its structure and function (1, 2). It consists of two chemically identical light chains which have different conformations: monomer 1 resembles the heavy chain, and monomer 2 the light chain of an Fab fragment. Each monomer consists of a variable and a constant domain connected by a switch peptide. In the crystal, the two variable domains, and also the two constant domains, have very similar structures related by local twofold axes. However, because the symmetry is only a local one, the surface of the domains is influenced by their different environments in the crystal.

The refinement of the Mcg Bence-Jones protein is in progress, using 12,500 reflections with $I > 5\ \sigma(I)$ from 6.5 to 2.3 Å. The refinement process started with the constrained crystallographic refinement of Deisenhofer and Steigemann (3). The positions of the atoms were improved by real-space refinement, followed by the calculation of structure factors and a new improved electron density map. This process was repeated cyclically, to the point of diminishing returns. At this stage, "manual" corrections were performed with the GRIP 75 molecular graphics system[1] at the University of North Carolina, using calculated Fourier and difference Fourier maps. At present, restrained least-squares refinement (4) is under way. The R-factor with overall temperature factor has now been decreased from the initial 43% to 26%.

As the refinement progressed, core segments of domains, which are expected to be identical, became increasingly similar. Upon superposition of $\alpha$-carbon positions of identical regular segments, the average deviation decreased from 0.95 to 0.4 Å. Fine points of the structure become evident; for example, the electron density distribution indicates that Pro 145 is a *cis* proline in both monomers. It is located in the third position of a reverse turn, as are *cis* prolines previously identified in other protein structures, including the variable domain of a $\kappa$ light chain (5). Proline 145 must be a structurally important residue, as the equivalent of Pro 145 is conserved in almost all constant region domains.

Initially, 360 atoms out of a total of 3,222 in the structure had no associated electron

---

[1]GRIP-75 developers included E. G. Britton, F. P. Brooks, Jr., J. Hermans, J. S. Lipscomb, J. E. McQueen, M. E. Pique, and W. V. Wright. GRIP-75 development has been supported by the National Institutes of Health Division of Research Resources, the National Science Foundation, the Atomic Energy Commission, and the International Business Machines Corporation.

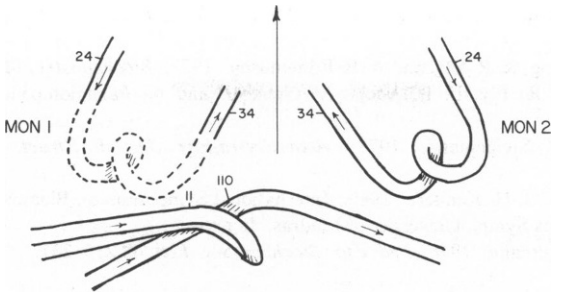


Figure 1 Schematic drawing of the first hypervariable regions of monomers 1 and 2, and of the chains of the neighboring molecule of the Mcg Bence-Jones dimer. Dashed lines indicate the section of monomer 1 that does not have electron density in the Fourier map. The position of the local twofold axis is shown by the arrow.

density, and were therefore not included in the calculations. Electron density for 200 of these atoms became visible during refinement. For each chain, there is still no density for some long side chains and for the first two N-terminal residues; also, the density is weak for the last two or three of the C-terminal residues. In monomer 1, the chain segments are visible up to residues 25 and 34, but eight residues (26–33, including the main chain) of the first hypervariable region have no associated density. In monomer 2, however, these eight residues form a well-defined helical segment. For both monomers, the conformations of the chain segment up to residues 24 and 35 are the same (the distances between the $\alpha$-carbon of 24 and the $\alpha$-carbon of 35 are 11.4 and 11.8 Å), but the relative positions of $\alpha$-carbons and side chain orientations of residues 25 and 34 are different in the two monomers.

In the crystal, chain segments of the neighboring molecule, including residues 7–11 and 106–110, come close to the missing region in monomer 1 (Fig. 1). To understand the influence of the neighboring molecule on this missing region, residues 25–34 of monomer 2 were transformed using the pseudo twofold axis where these residues should be in monomer 1. The distances between the neighboring molecule and the transformed segment were then calculated. The main chain (carbonyl oxygen of 31 and $\alpha$-carbon of 32) is <3 Å from the main chain of residue 11 (carbonyl oxygen). Also, side chain atoms of Tyr 32 come too close to the side chain and main chain of residues 9–11, and the side chain of Tyr 34 is too close to side chains of residues 108–110. Because of the above space limitations, residues 25–34 in monomer 1 cannot have the conformation they have in monomer 2.

The lack of electron density for the residues 26–33 of monomer 1 is apparently caused by the distorting effect of the lattice forces from the close approach of the neighboring molecule. The effects of the distortion are non-uniform, giving rise to a number of less favorable conformations, and causing the apparent disorder in this region. The lattice forces do not seem to affect the molecule making the close approach, since the electron densities of its contacting residues are well defined.

Residues 25–34 of both monomers are in the hypervariable region and form part of the antibody binding site. Considering possible allosteric mechanisms of antigen binding to attain optimal antibody-antigen complementarity, it may be significant that this chain segment can be altered with relative ease.

This work is supported by the U. S. Department of Energy under contract W-31-109-ENG-38.

*Received for publication 15 December 1979.*

REFERENCES

1. Schiffer, M., R. L. Girling, K. R. Ely, and A. B. Edmundson. 1973. *Biochemistry.* **12**:4620–4631.
2. Edmundson, A. B., K. R. Ely, E. E. Abola, M. Schiffer, and N. Panagiotopoulos. 1975. *Biochemistry.* **14**:3953–3961.
3. Deisenhofer, J., and W. Steigemann. 1975. *Acta Crystallogr. Sect. B. Struct. Crystallogr. Cryst. Chem.* **31**:238–250.
4. Hendrickson, W. A., and J. H. Konnert. 1980. International Symposium on Biomolecular Structure, Function, and Evolution. Madras Symp., University of Madras. In press.
5. Huber, R., and W. Steigemann. 1976. *Fed. Eur. Biochem. Soc. Lett.* **48**:235–237.

# A NEW METHOD FOR DETERMINING PROTEIN SECONDARY STRUCTURE BY LASER RAMAN SPECTROSCOPY APPLIED TO fd PHAGE

R. W. Williams and A. K. Dunker, *Biochemistry/Biophysics Program, Washington State University, Pullman, Washington 99164*
W. L. Peticolas, *Chemistry Department, University of Oregon, Eugene, Oregon 97403 U.S.A.*

## INTRODUCTION

A new method is presented for estimating the secondary structure of proteins from the intensity distribution of the laser Raman amide I spectrum. We have applied this method to the coat protein of the fd filamentous phage.

At a fixed frequency, the observed Raman scattering intensity for a single protein may be expressed as $f_{ho}I_{ho} + f_{hd}I_{hd} + f_{ba}I_{ba} + f_{\beta p}I_{\beta p} + f_tI_t + f_uI_u = Ie$, where $Ie$ is the normalized experimental Raman intensity, each $f$ is the fraction of a type of secondary structure and each $I$ is the intensity that would be observed for a polypeptide with 100% of the indicated structure type. The structure types are: *ho*, ordered helix; *hd*, disordered helix; $\beta a$, antiparallel $\beta$-sheet; $\beta p$, parallel $\beta$-sheet; *t*, turn; and *u*, undefined. The experimental Raman intensity is normalized by dividing the observed intensity at each wavenumber by the sum over all wavenumbers of the observed intensities.

## METHODS

Laser Raman spectra of the proteins listed in Table I were collected and solvent spectra were substracted generally as described elsewhere (Dunker et al., 1979).

Six reference intensities, $I$, representing the spectra of polypeptides with a single structure type, were computed from eleven equations, each equation representing a different protein of known structure. This set of solutions provides the reference spectra.

Linear combinations of the reference spectra were then fitted to the amide I spectrum of each protein for which an estimate of structure, $f$, was desired.

In our calculations of reference spectra, we have relied on the x-ray diffraction derived estimates of secondary structure obtained by Levitt and Greer (1977) or on the references therein. We have made a distinction between central helical residues that are likely to be hydrogen bonded at both the amide hydrogen and at the carbonyl oxygen (ordered helix) and end residues that have only one hydrogen bond (disordered helix).

## RESULTS

Results are shown in Table I.